Electronic Supporting Material

Single-molecule magnets within polyoxometalate-based frameworks

Malihe Babaei Zarch [a], Masoud Mirzaei [a,*], Maryam Bazargan [a], Sandeep K. Gupta[b], Franc Meyer [b], and Joel T. Mague [c]

[a] *Department of Chemistry, Faculty of Science, Ferdowsi University of Mashhad, Mashhad 9177948974, Iran. E-mail: mirzaeesh@um.ac.ir*

[b] *Institut für Anorganische Chemie, Georg-August-Universität Göttingen, Tammannstrasse 4, 37077 Göttingen, Germany*

[c] *Department of Chemistry, Tulane University, New Orleans, LA, 70118, USA*

Contents

Figure S1. XRD patterns of **1** and **2** (simulated and experimental). 2

Figure S2. FTIR spectra of **1**, **2** and $H_4[(SiO_4)@W_{12}O_{36}]$. 2

Figure S3. TGA curves for hybrids **1** and **2**. 3

Figure S4. Hydrogen bonding patterns between surface oxygen atoms of the Keggin anion and neighbouring cationic layers of **1**. Color code: Ho, green; C, light grey; N, dark blue; O, red; W, blue; Si, pale yellow; H, white. 4

Figure S5. Hydrogen bonding patterns between surface oxygen atoms of the Keggin anion and neighbouring cationic layers of **2**. Color code: Tb, green; C, light grey; N, dark blue; O, red; W, blue; Si, pale yellow; H, white. 5

Figure S6. Plots of the reduced magnetization *M* versus *H*/*T* in the field range 0-7 T and temperature range 2.0-10.0 K for **1**. 6

Figure S7. Field dependence of the magnetization for compound **2** at indicated temperatures. 6

Figure S8. Plots of the reduced magnetization *M* versus *H*/*T* in the field range 0-7 T and temperature range 2.0-10.0 K for **2**. 7

Figure S9. Temperature dependence of the in-phase (a) and out-of-phase (b) components of the ac susceptibility for **1** under zero dc field. 8

Figure S10. Temperature dependence of the in-phase (a) and out-of-phase (b) components of the ac susceptibility for **2** under zero dc field. 9

Figure S11. Temperature dependence of the in-phase component of the ac susceptibility for complex **2** under an applied dc field of 1500 Oe. 10

Figure S12. Temperature dependence of the out-of-phase component of the ac susceptibility for complex **2** under an applied dc field of 1500 Oe. 11

Table S1: Selected bond lengths [Å] and angles (°) for hybrids **1** and **2**. 12

Table S2: Hydrogen-bond geometry (Å, °) for hybrid **1**. 13

Table S3: Hydrogen-bond geometry (Å, °) for hybrid **2**. 14

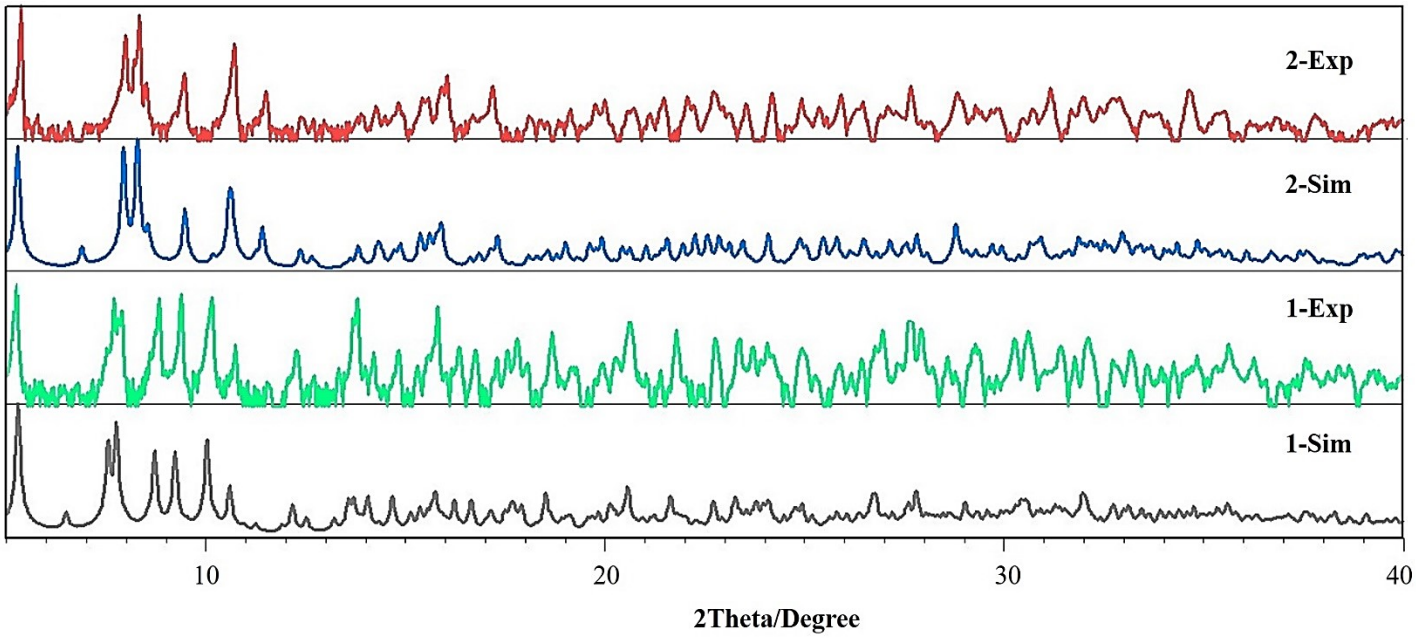

Figure S1. XRD patterns of **1** and **2** (simulated and experimental).

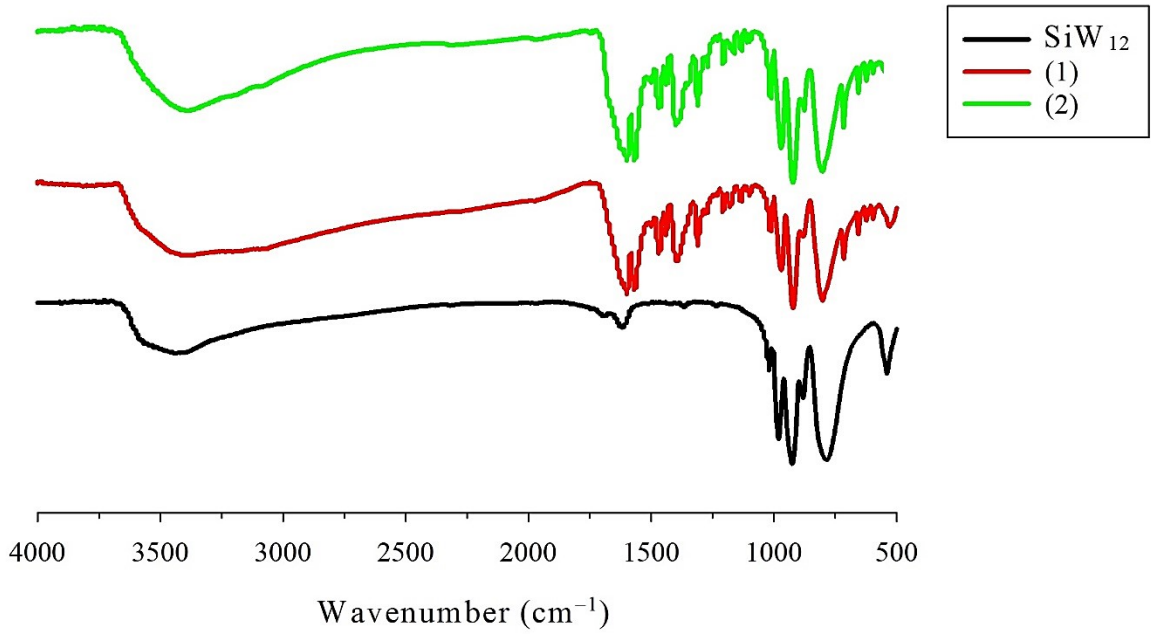

Figure S2. FTIR spectra of **1**, **2** and $H_4[(SiO_4)@W_{12}O_{36}]$.

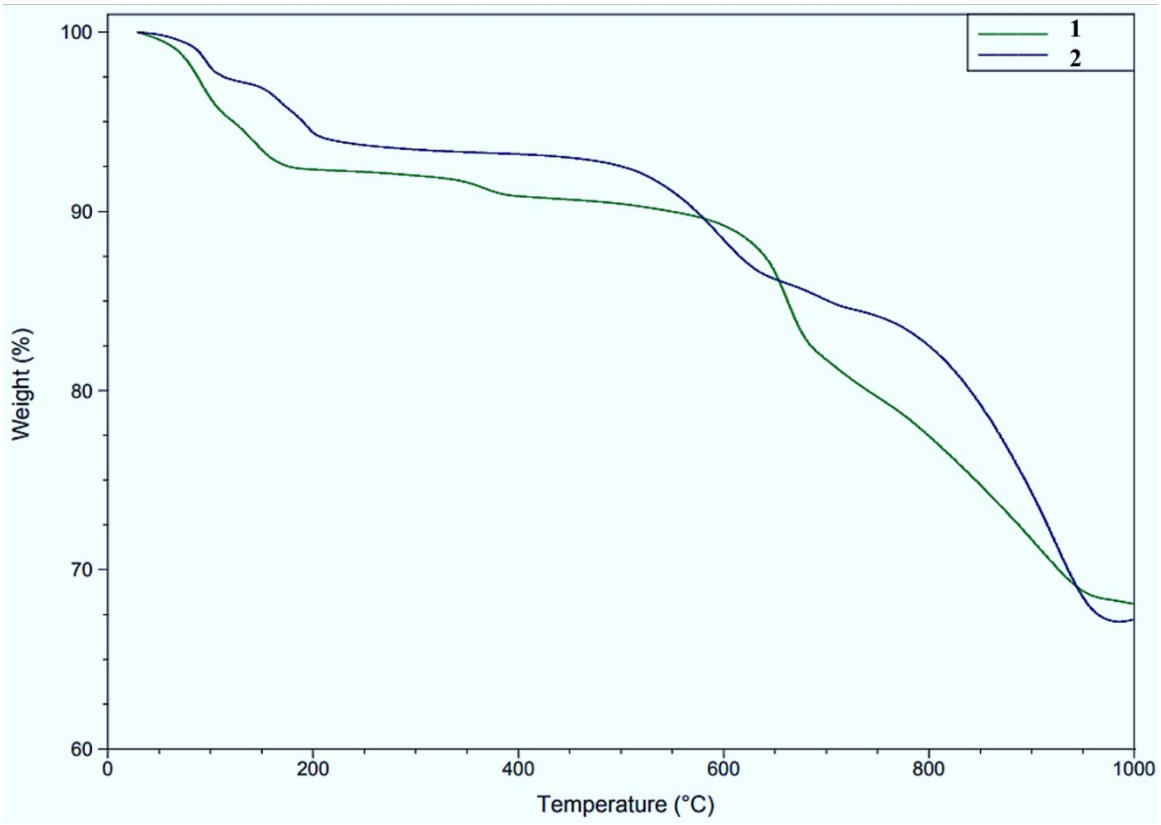

Figure S3. TGA curves for hybrids **1** and **2**.

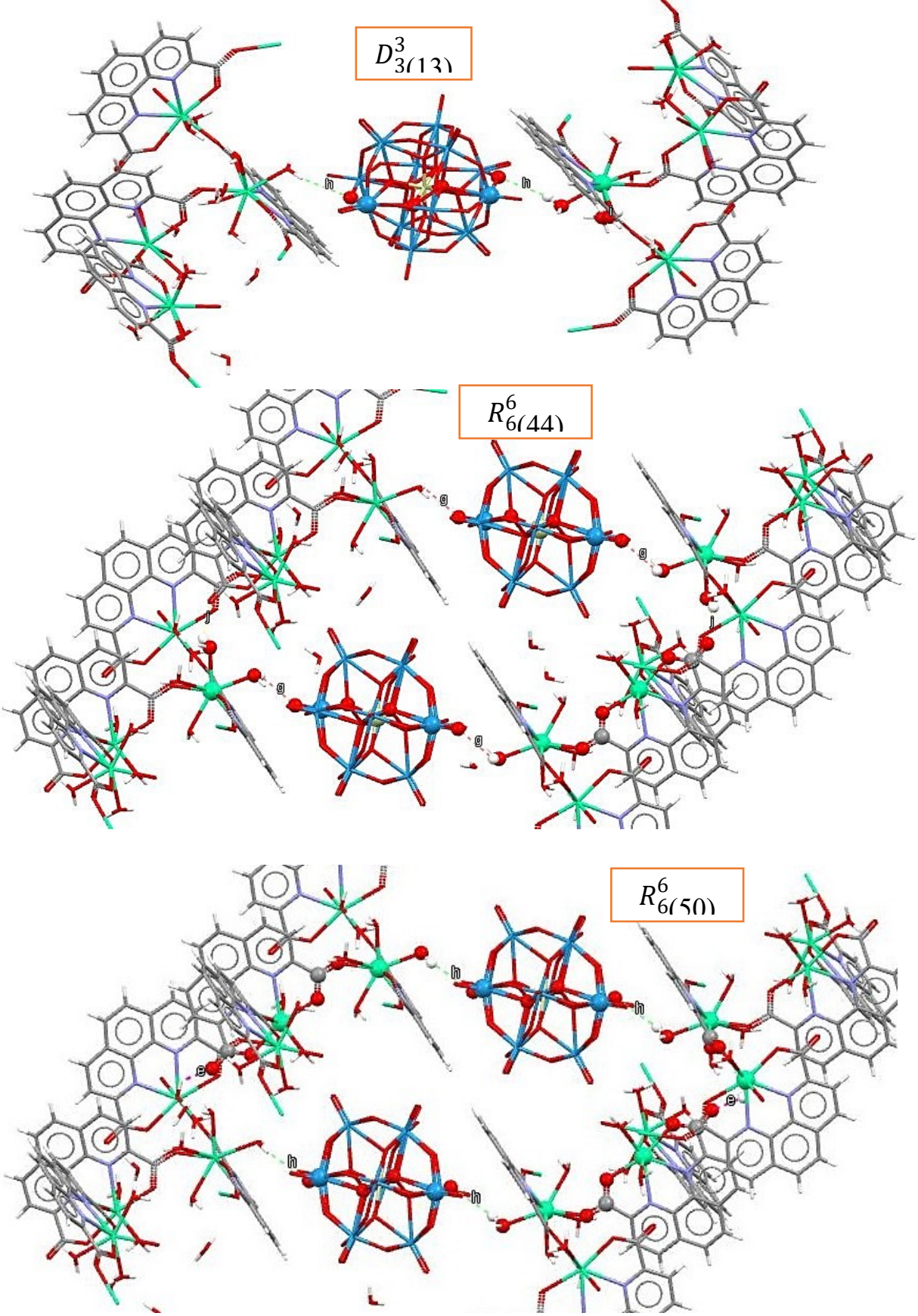

Figure S4. Hydrogen bonding patterns between surface oxygen atoms of the Keggin anion and neighbouring cationic layers of **1**. Color code: Ho, green; C, light grey; N, dark blue; O, red; W, blue; Si, pale yellow; H, white.

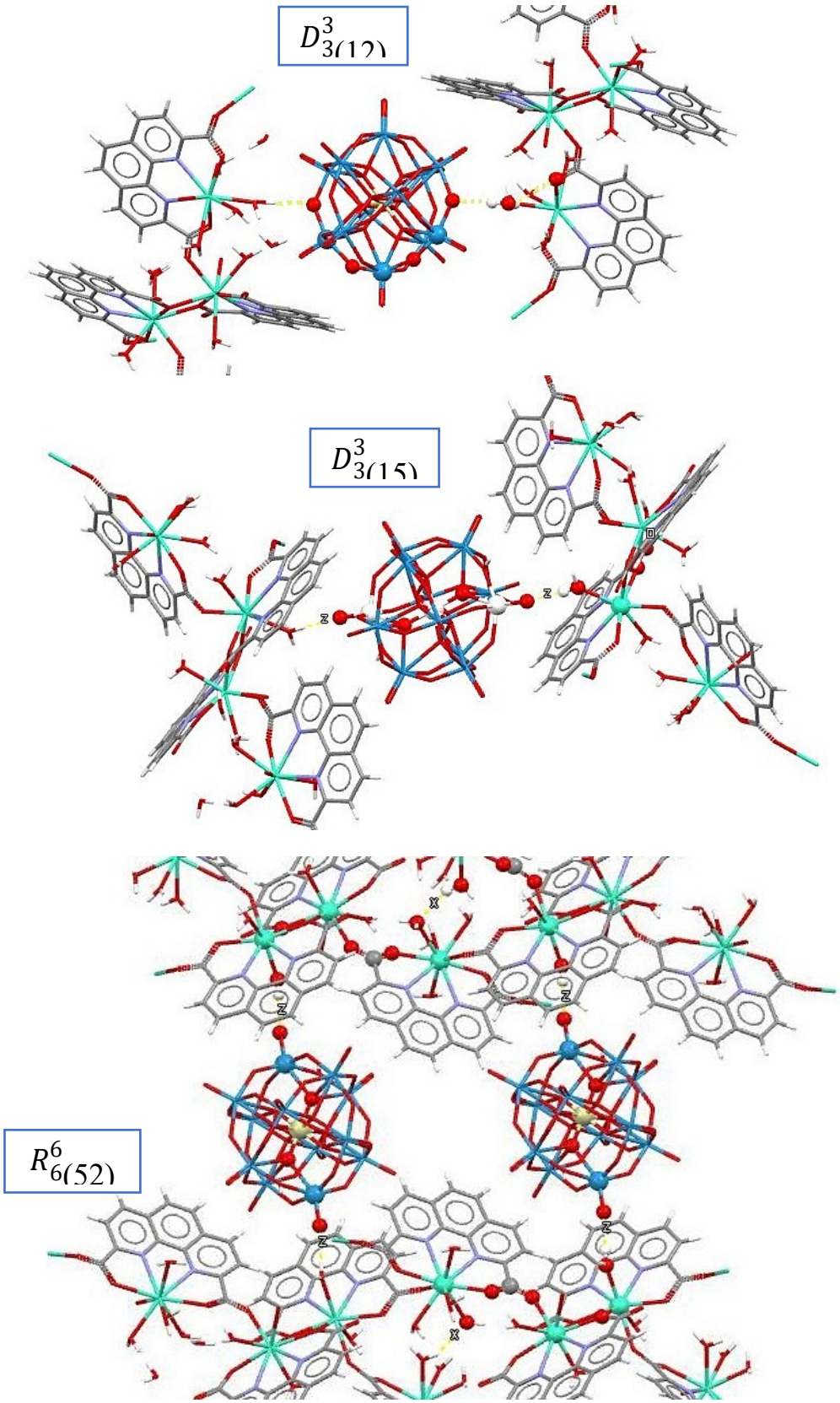

Figure S5. Hydrogen bonding patterns between surface oxygen atoms of the Keggin anion and neighbouring cationic layers of **2**. Color code: Tb, green; C, light grey; N, dark blue; O, red; W, blue; Si, pale yellow; H, white.

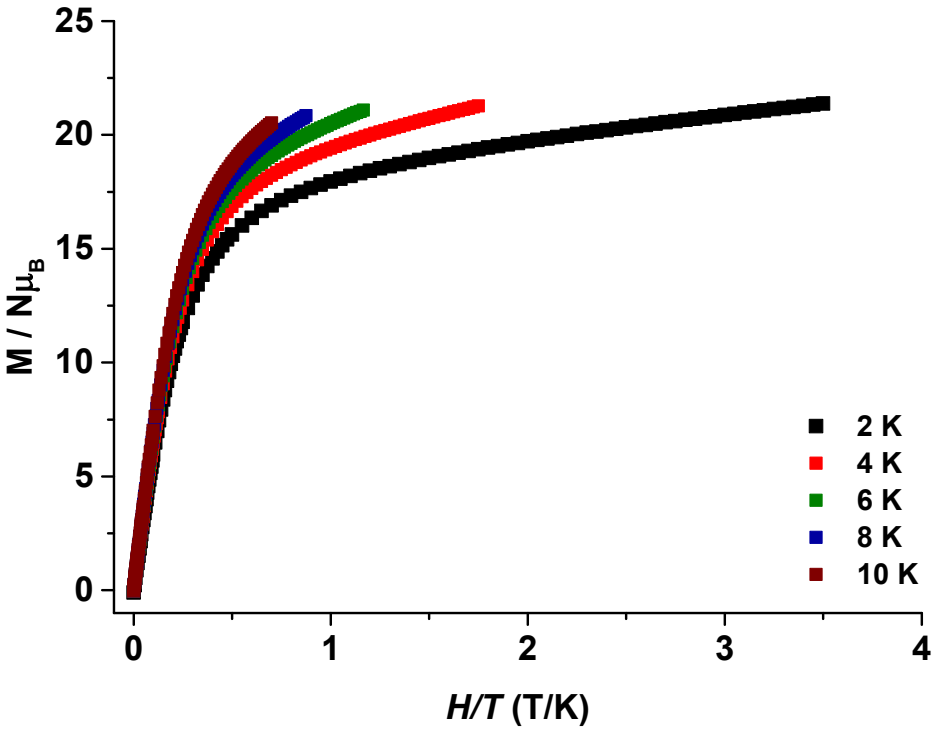

Figure S6. Plots of the reduced magnetization *M* versus *H*/*T* in the field range 0-7 T and temperature range 2.0-10.0 K for **1**.

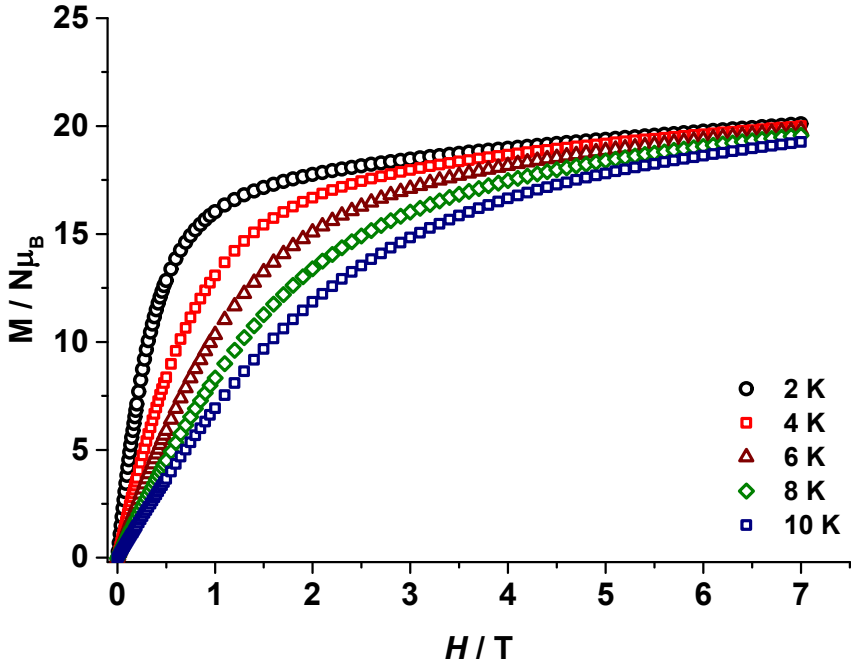

Figure S7. Field dependence of the magnetization for compound **2** at indicated temperatures.

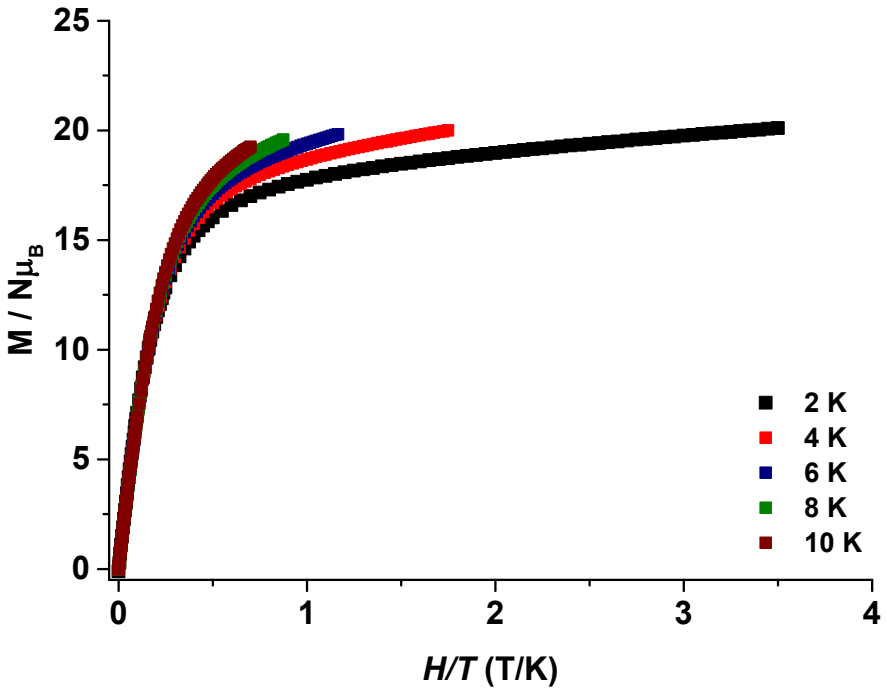

Figure S8. Plots of the reduced magnetization *M* versus *H*/*T* in the field range 0-7 T and temperature range 2.0-10.0 K for **2**.

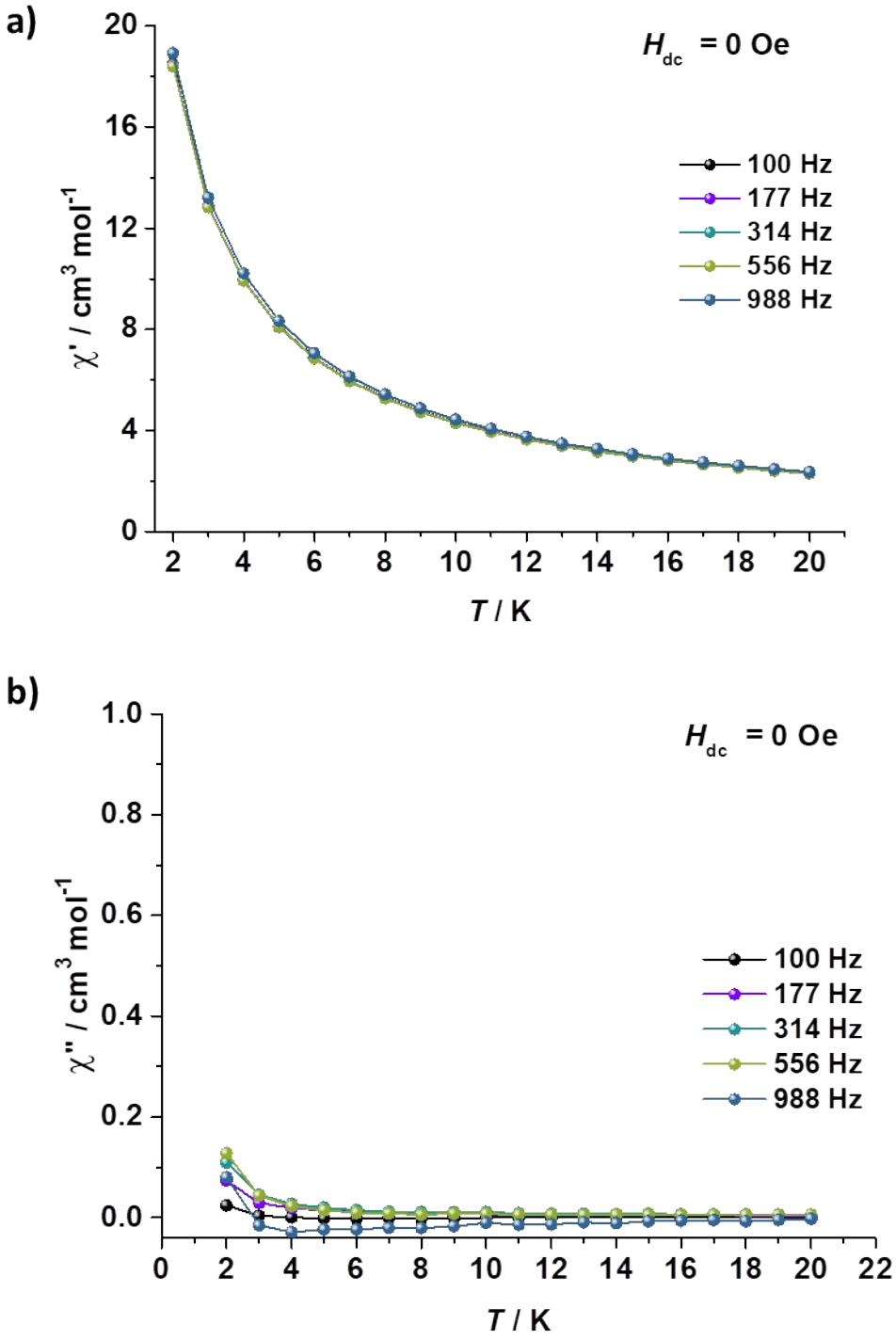

Figure S9. Temperature dependence of the in-phase (a) and out-of-phase (b) components of the ac susceptibility for **1** under zero dc field.

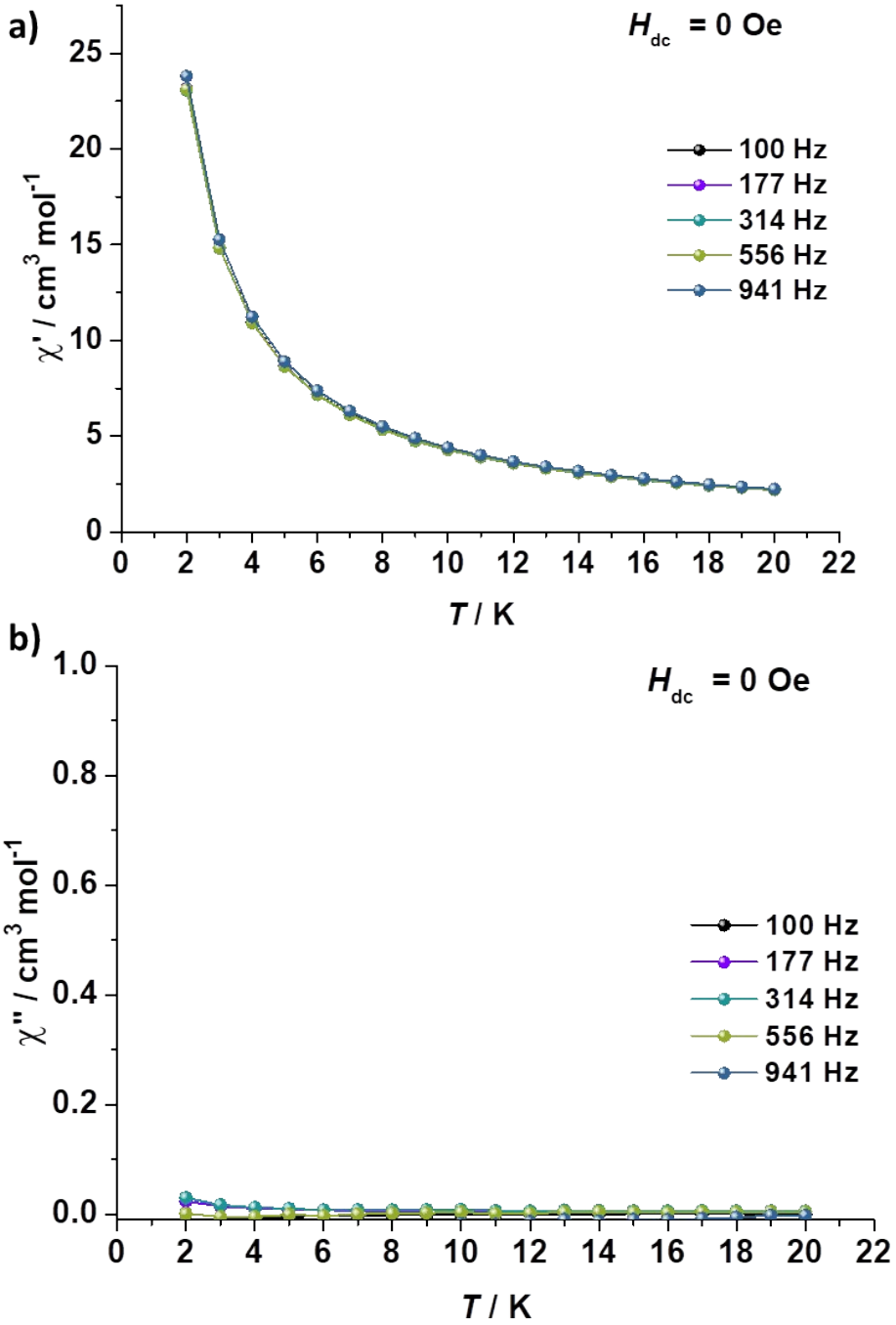

Figure S10. Temperature dependence of the in-phase (a) and out-of-phase (b) components of the ac susceptibility for **2** under zero dc field.

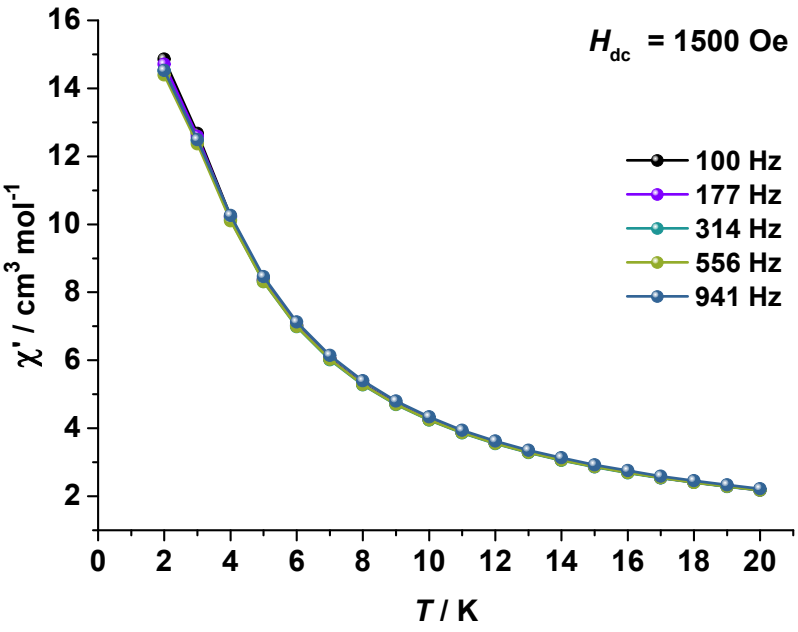

Figure S11. Temperature dependence of the in-phase component of the ac susceptibility for complex **2** under an applied dc field of 1500 Oe.

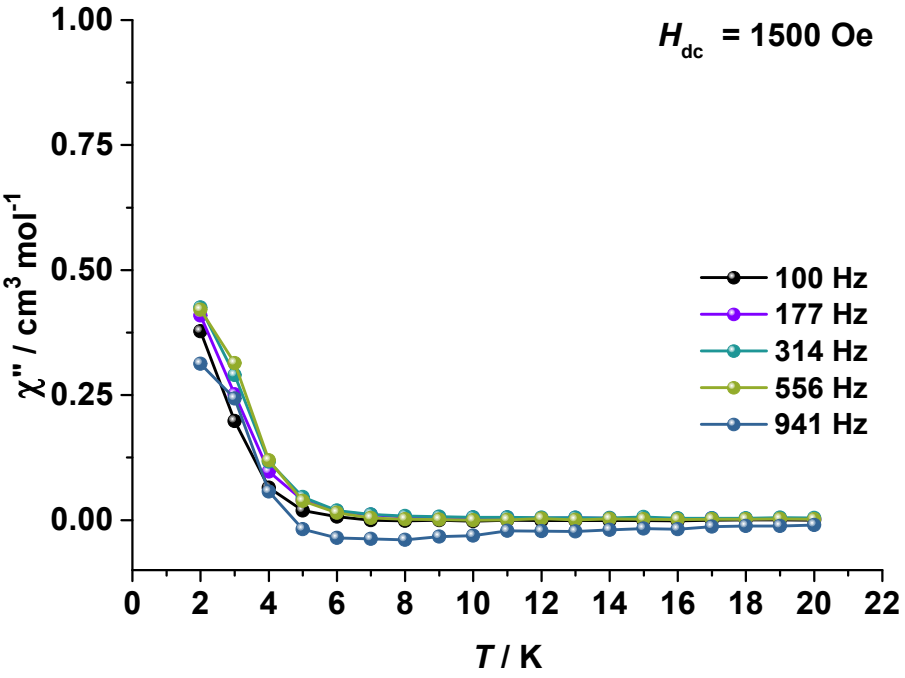

Figure S12. Temperature dependence of the out-of-phase component of the ac susceptibility for complex **2** under an applied dc field of 1500 Oe.

Table S1: Selected bond lengths [Å] and angles (°) for hybrids **1** and **2**.

Hybrids		$Ln–O_{Carboxylate}$	Ln–N	$Ln–O_{Water}$	N–Ln–N
1	Ho1	2.327 (7) 2.345 (8) 2.285 (7) 2.369 (7)	2.455 (7) 2.490 (7)	2.390 (7) 2.324 (7)	64.48 (2)
	Ho2	2.378 (7) 2.341 (7) 2.360 (7)	2.474 (7) 2.506 (7)	2.341 (6) 2.351 (7) 2.315 (8)	63.57 (2)
	Ho3	2.332 (7) 2.372 (7) 2.336 (6) 2.323 (7)	2.458 (7) 2.473 (7)	2.359 (7) 2.337 (7)	64.76 (2)
	Ho4	2.350 (1) 2.456 (7) 2.372 (7)	2.498 (7) 2.518 (7)	2.360 (8) 2.347 (8) 2.400 (8) 2.550 (1)	63.66 (2)
2	Tb1	2.44 (1) 2.42 (2) 2.41 (1)	2.530 (2) 2.520 (1)	2.560 (2) 2.440 (2) 2.400 (2) 2.400 (2)	62.83 (5)
	Tb2	2.331 (1) 2.436 (1) 2.410 (1) 2.520 (1) 2.482 (1)	2.536 (1) 2.558 (1)	2.432 (1) 2.414 (1)	63.37 (4)
	Tb3	2.396 (1) 2.279 (1)	2.501 (1) 2.465 (1)	2.380 (1) 2.350 (1)	63.60 (4)
	Tb4	2.344 (2) 2.396 (1)	2.507 (1) 2.505 (1)	2.402 (1) 2.383 (2) 2.446 (1) 2.497 (2)	63.41 (4)

Table S2: Hydrogen-bond geometry (Å, °) for hybrid **1**.

D–H···A	D–H	H···A	D···A	D–H···A
O7–H7A···O49	0.87	2.06	2.811 (10)	143
O10–H10A···O14	0.87	1.88	2.657 (9)	148
O11–H11A···O83^{i}	0.91	2.08	2.98 (3)	171
O11–H11B···O16^{ii}	0.91	1.80	2.672 (10)	162
O12–H12B···O79^{iii}	0.90	2.07	2.812 (19)	139
O18–H18A···O77^{iii}	0.88	2.09	2.743 (16)	130
O18–H18A···O80^{iii}	0.88	2.64	3.438 (18)	151
O19–H19A···O2^{iv}	0.89	2.29	2.939 (11)	130
O19–H19B···O21	0.89	1.81	2.678 (10)	166
O24–H24A···O52^{v}	0.88	2.57	3.143 (13)	123
O25–H25A···O78	0.88	2.10	2.706 (15)	126
O25–H25B···O2^{iv}	0.88	2.10	2.793 (13)	135
O26–H26A···O71	0.87	2.16	2.79 (2)	128
O27–H27A···O83	0.91	1.83	2.49 (3)	128
C3–H3···O32^{i}	0.95	2.44	3.338 (13)	158
C24–H24···O49^{vi}	0.95	2.60	3.550 (13)	177
C37–H37···O82^{iii}	0.95	2.23	3.159 (12)	165
C44–H44···O77^{iii}	0.95	2.42	3.31 (2)	157
O71–H71B···O49	0.87	2.35	3.22 (2)	174
O72–H72A···O52	0.87	2.29	3.046 (16)	146
O72–H72B···O29^{vii}	0.87	2.01	2.878 (15)	174
O74–H74B···O7	0.87	2.14	3.01 (2)	177
O76–H76B···O31	0.87	2.61	3.17 (2)	124
O77–H77B···O78	0.87	1.84	2.66 (2)	156
O80–H80B···O10^{viii}	0.87	2.47	3.130 (17)	134
O81–H81B···O72	0.87	2.04	2.730 (17)	135
O82–H82A···O12^{vi}	0.87	1.87	2.709 (10)	162
O82–H82B···O14^{vi}	0.87	2.10	2.831 (11)	141

Symmetry codes: (i) −*x*+3/2, *y*+1/2, −*z*+1/2; (ii) *x*+1, *y*, *z*; (iii) −*x*+1/2, *y*+1/2, −*z*+1/2; (iv) *x*−1, *y*, *z*; (v) −*x*+1, −*y*+1, −*z*+1; (vi) −*x*+3/2, *y*−1/2, −*z*+1/2; (vii) −*x*+1, −*y*, −*z*+1; (viii) −*x*+1/2, *y*−1/2, −*z*+1/2.

Table S3: Hydrogen-bond geometry (Å, °) for hybrid **2**.

D–H···A	D–H	H···A	D···A	D–H···A
O4–H4A···O74	0.87	2.11	2.97 (6)	168
O4–H4B···O11	0.87	2.37	3.14 (2)	147
O5–H5A···O75	0.87	1.96	2.83 (2)	178
O5–H5B···O72	0.87	2.28	3.03 (2)	145
O6–H6A···O72	0.87	1.79	2.66 (2)	176
O6–H6B···O20^{i}	0.87	2.19	2.78 (2)	125
O6–H6B···O27^{i}	0.87	2.42	3.21 (3)	152
O8–H8A···O73	0.87	1.94	2.81 (3)	176
O8–H8B···O75	0.87	2.51	3.20 (2)	138
O15–H15A···O1	0.87	1.72	2.59 (2)	180
O15–H15B···O30^{ii}	0.87	2.17	2.810 (18)	130
O16–H16A···O28	0.87	1.90	2.736 (18)	160
O16–H16B···O21	0.87	2.30	3.02 (2)	140
O19–H19A···O22	0.87	1.94	2.779 (19)	161
O19–H19B···O52^{iii}	0.87	2.11	2.94 (2)	159
O24–H24A···O74^{iii}	0.87	2.16	3.01 (7)	168
O24–H24B···O67^{iv}	0.87	2.42	3.17 (2)	146
O25–H25A···O74^{iii}	0.87	2.32	3.18 (8)	168
O26–H26A···O7^{v}	0.87	1.84	2.712 (18)	180
O26–H26B···O33	0.87	2.17	2.861 (17)	137
O27–H27A···O4^{iii}	0.87	2.10	2.97 (3)	179
O27–H27B···O20	0.87	2.22	3.02 (3)	153
O76–H76A···O14^{vi}	0.87	1.91	2.780 (18)	180
O76–H76B···O55^{iv}	0.87	2.01	2.882 (17)	175

Symmetry codes: (i) x, y−1, z; (ii) −x, y−1/2, −z+1/2; (iii) x, y+1, z; (iv) −x+1, −y+1, −z+1; (v) x, −y+1/2, z+1/2; (vi) x, −y+3/2, z+1/2.